(12)

VSC-TR-82-5

ANALYSIS OF TECHNIQUES FOR APPLICATION OF MAGNITUDE CORRECTIONS DEVELOPED BY MARSHALL, SPRINGER, AND RODEAN

Robert R. Blandford and Zoltan A. Der

Seismic Data Analysis Center
Teledyne Geotech
314 Montgomery Street
Alexandria, Virginia 22314

12 NOV 1981

APPROVED FOR PUBLIC RELEASE; DISTRIBUTION UNLIMITED.

Monitored By:
VELA Seismological Center
312 Montgomery Street
Alexandria, VA 22314

Unclassified

SECURITY CLASSIFICATION OF THIS PAGE (When Data Entered)

REPORT DOCUMENTATION PAGE

READ INSTRUCTIONS BEFORE COMPLETING FORM

1. REPORT NUMBER VSC-TR-82-5 / 2. GOVT ACCESSION NO. AD-A117 402	3. RECIPIENT'S CATALOG NUMBER
4. TITLE (and Subtitle) ANALYSIS OF TECHNIQUES FOR APPLICATION OF MAGNITUDE CORRECTIONS DEVELOPED BY MARSHALL, SPRINGER AND RODEAN	5. TYPE OF REPORT & PERIOD COVERED Technical 6. PERFORMING ORG. REPORT NUMBER SDAC-TR-81-13
7. AUTHOR(s) Robert R. Blandford Z. A. Der	8. CONTRACT OR GRANT NUMBER(s) F08606-79-C-0007
9. PERFORMING ORGANIZATION NAME AND ADDRESS Teledyne Geotech 314 Montgomery Street Alexandria, Virginia 22314	10. PROGRAM ELEMENT, PROJECT, TASK AREA & WORK UNIT NUMBERS VT/0709/B/PMP
11. CONTROLLING OFFICE NAME AND ADDRESS VELA Seismological Center 312 Montgomery Street Alexandria, Virginia 22314	12. REPORT DATE 11/12/81 13. NUMBER OF PAGES 38
14. MONITORING AGENCY NAME & ADDRESS(if different from Controlling Office) Defense Advanced Research Projects Agency 1400 Wilson Boulevard Arlington, Virginia 22209	15. SECURITY CLASS. (of this report) Unclassified 15a. DECLASSIFICATION/DOWNGRADING SCHEDULE

16. DISTRIBUTION STATEMENT (of this Report)

APPROVED FOR PUBLIC RELEASE; DISTRIBUTION UNLIMITED.

17. DISTRIBUTION STATEMENT (of the abstract entered in Block 20, if different from Report)

18. SUPPLEMENTARY NOTES

Author's Report Date 23 March 1981

19. KEY WORDS (Continue on reverse side if necessary and identify by block number)

m_b	t*
Yield	pP
Q	Station Corrections

20. ABSTRACT (Continue on reverse side if necessary and identify by block number)

Analysis of the procedures recommended by Marshall, Springer and Rodean (1979) for correction of explosion magnitude due to pP and absorption shows that the techniques are needed and are generally satisfactory. However, the pP correction could be made more accurate and operationally applicable, and the absorption correction needs further checking and perhaps a different approach. A new attack on the general problem is recommended in order to properly treat problems of focusing-defocusing, crustal amplification, clipping and noise data, and pP and absorption as mentioned above.

DD FORM 1 JAN 73 1473 EDITION OF 1 NOV 65 IS OBSOLETE

Unclassified

SECURITY CLASSIFICATION OF THIS PAGE (When Data Entered)

ANALYSIS OF TECHNIQUES FOR APPLICATION OF MAGNITUDE CORRECTIONS DEVELOPED BY MARSHALL, SPRINGER AND RODEAN

SEISMIC DATA ANALYSIS CENTER REPORT NO.: SDAC-TR-81-13

AFTAC Project Authorization No.:	VELA VT/0709/B/PMP
Project Title:	Seismic Data Analysis Center
ARPA Order No.:	2551
Name of Contractor:	TELEDYNE GEOTECH
Contract No.:	F08606-79-C-0007
Date of Contract:	01 October 1979
Amount of Contract:	$2,191,475
Contract Expiration Date:	30 September 1983
Project Manager:	Robert R. Blandford (703) 836-3882

P. O. Box 334, Alexandria, Virginia 22313

APPROVED FOR PUBLIC RELEASE; DISTRIBUTION UNLIMITED.

ABSTRACT

Analysis of the procedures recommended by Marshall, Springer and Rodean (1979) for correction of explosion magnitude due to pP and absorption shows that the techniques are needed and are generally satisfactory. However, the pP correction could be made more accurate and operationally applicable, and the absorption correction needs further checking and perhaps a different approach. A new attack on the general problem is recommended in order to properly treat problems of focusing-defocusing, crustal amplification, clipping and noise data, and pP and absorption as mentioned above.

TABLE OF CONTENTS

LIST OF FIGURES

LIST OF FIGURES (Continued)

INTRODUCTION

A recent paper by Marshall, Springer and Rodean (1979), hereafter referred to as MSR, has presented a comprehensive procedure for calculating yields from short-period body wave magnitude. In that report, they give procedures for correcting the magnitude for effects of source and receiver absorption, pP, and station effects. The principal objective of this report is to evaluate their procedures for absorption and pP corrections.

Attenuation Correction

The basic approach in MSR is to determine mantle Q under inaccessible locations. While the magnitude and spectral measurements need for determining Q are not available in most regions, detailed crustal surveys that include values of P_n velocities have been published for areas of the Soviet Union, China, South Africa, etc. MSR use the apparently good correlation between P_n velocities and the residuals of Booth et al. (1974) to predict m_b residuals for the rest of the world. While the idea is attractive, more work is needed to establish the validity of such a correlation worldwide. The residuals of Booth et al. (1974) are not corrected for crustal effects. It has been found that such corrections, while somewhat inaccurate, can be used to reduce the variance in m_b station biases (Der et al., 1979). Beside the lack of crustal corrections, there is considerable variation among the various studies of magnitude biases for the same set of stations and the neat correlation that is displayed by MSR may not exist. Another possible objection to MSR's procedure is that the physical basis for causal interrelationship between P_n velocity and mantle attenuation is somewhat shaky. The P_n velocity is determined by the uppermost mantle, the so called "lid zone", while the magnitude bias is caused by losses in the total thickness of the upper mantle. Nevertheless, there may be a causal link; portions of the mantle with low Q are probably hot, which causes lowering of the P_n velocity. However, compositional changes are also necessary to explain the range of P_n velocities under the United States.

In order to test the validity of Q corrections derived from P_n data we have corrected the residuals of Booth et al for crustal effects using the results in Der et al. (1979) and plotted the corrected m_b terms against P_n velocities. The resulting plot is shown in Figure 2. The line of Marshall et al is superposed, but is shifted down .12 magnitude units since we reduced our m_b to that of a granite station, making our crustal corrections negative. The data points are suggestive of a curve that is similar in shape to that presented in Marshall et al. If averages for each P_n velocity interval are used, the resulting data points and curve are not dissimilar to those in Figure 1. This shows that the application of crustal station corrections does not alter the conclusions of MSR.

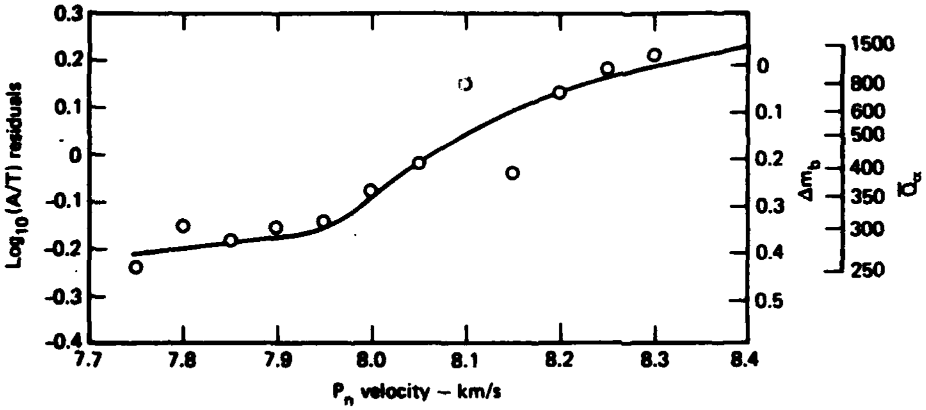

Figure 1. Observed relationship between P_n and $\log_{10}(A/T)$ residuals, comparison with calculated Δm_b corrections and Q_α for T = 0.75s (from Marshall et al, 1979).

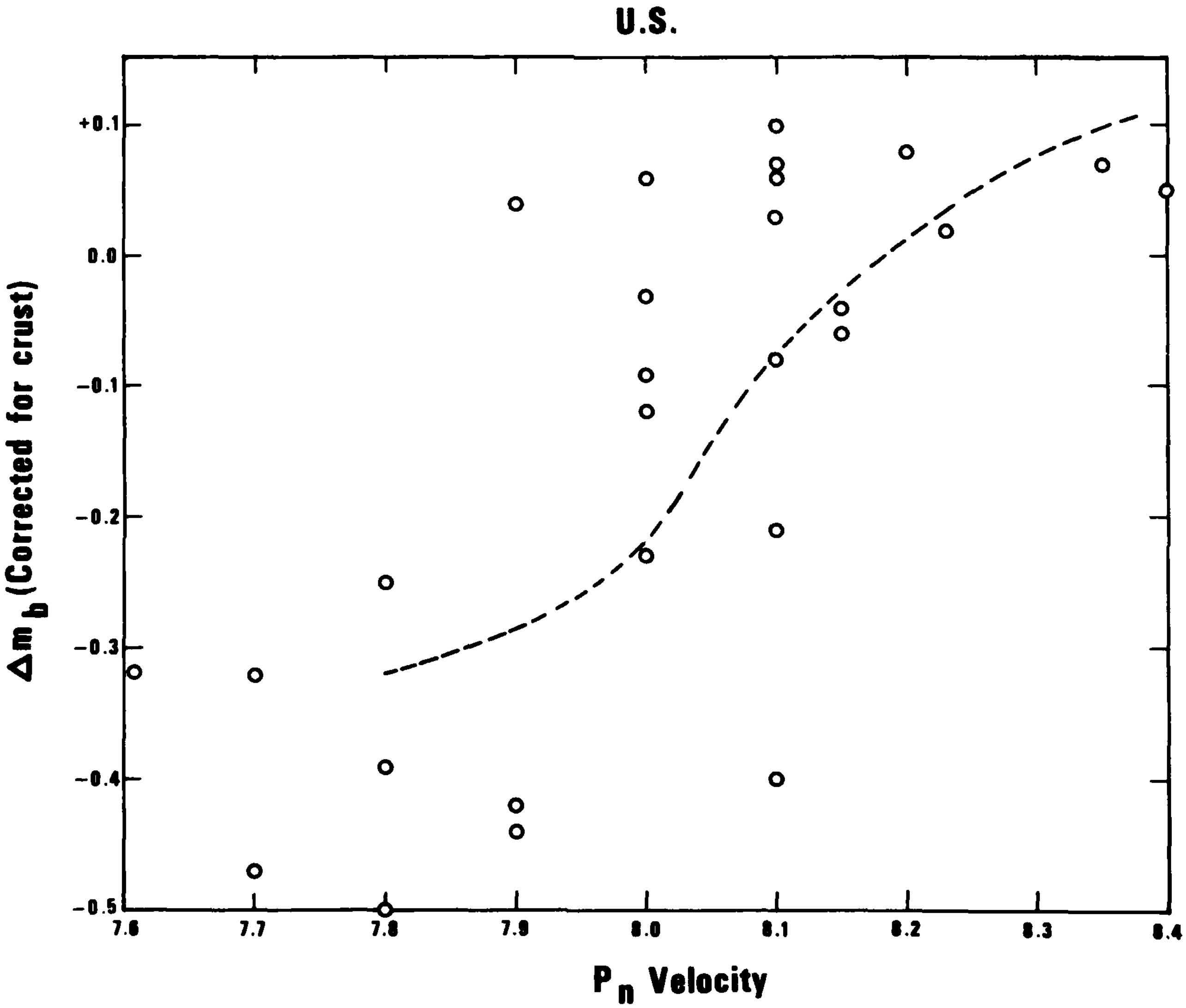

Figure 2. LRSM magnitude residuals from Booth et al (1974) with crustal corrections due to Der et al (1979) as a function of P_n velocity as from Marshall et al (1979). The curve drawn is from Marshall et al adjusted down by 0.12 to allow for the crustal corrections.

Let us now examine the worldwide validity of this relationship by plotting the m_b bias terms of North (1977) against the P_n values listed by MSR (see Figure 3). The bias terms are not corrected for the crust, since such correction terms are not available. The MSR data set is dificient in stations which have low P_n velocity. In order to correct this deficiency, we have added some African stations (BHA, MTD, KRR, CLK and CIR). We assume that the P_n velocity for these was 7.95 as given by Searle and Gouin (1971). It must also be pointed out that even lower P_n velocities are suggested by Dopp (1964) in the western rift zone. Again, superposing the curve of Marshall et al resutls in a strong suggestion that P_n velocities and magnitude biases are correlated worldwide in the manner presented in their paper.

The U.S. WWSSN stations also show a correlation between P_n velocity and magnitude bias terms similar to the LRSM data set (Figure 4, after North, 1977).

In summary, we can find no empirical fault with the procedure of Marshall et al., although its theoretical foundation is slightly shaky.

Before the procedure is adapted for general use it would perhaps be advisable to extend the existing m_b-bias, P_n velcoity data set to test the general validity of such relationships. In our view, data points in the foldbelts surrounding the Eurasian landmass are crucial and can be obtained without acquiring new data besides the WWSSN and the SRO network. In addition, other indirect methods suing other types of independent geophysical variables, e.g., travel time delays and spectral anomalies also need to be tested. Finally, the defining relationship for absorption is the spectral ratios of common events at different stations and these should be computed to the extent data are available.

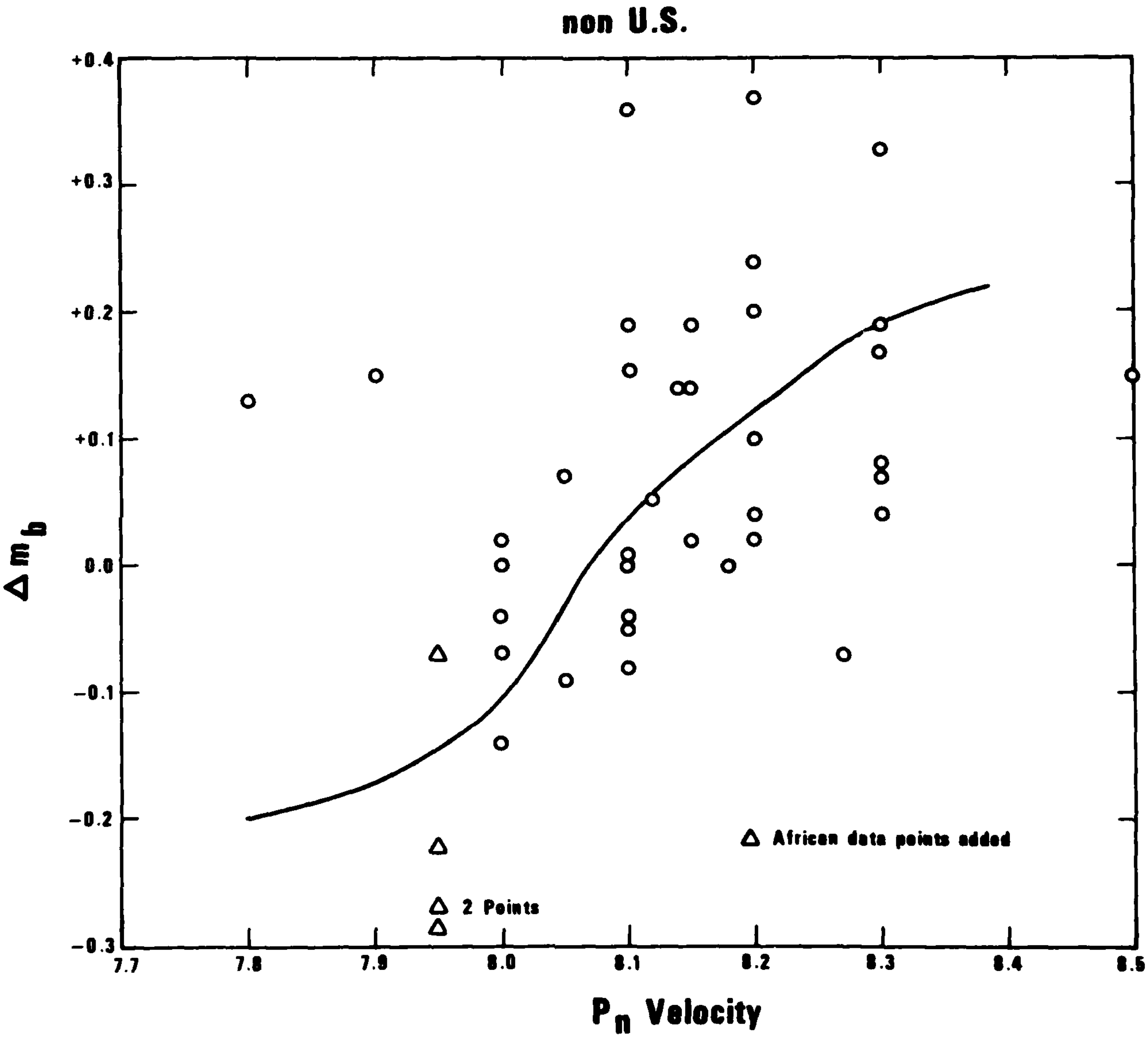

Figure 3. Magnitude residuals of North (1977) plotted as a function of P_n velocity due to Marshall et al (1979). The superimposed line is, again, due to Marshall et al (1979).

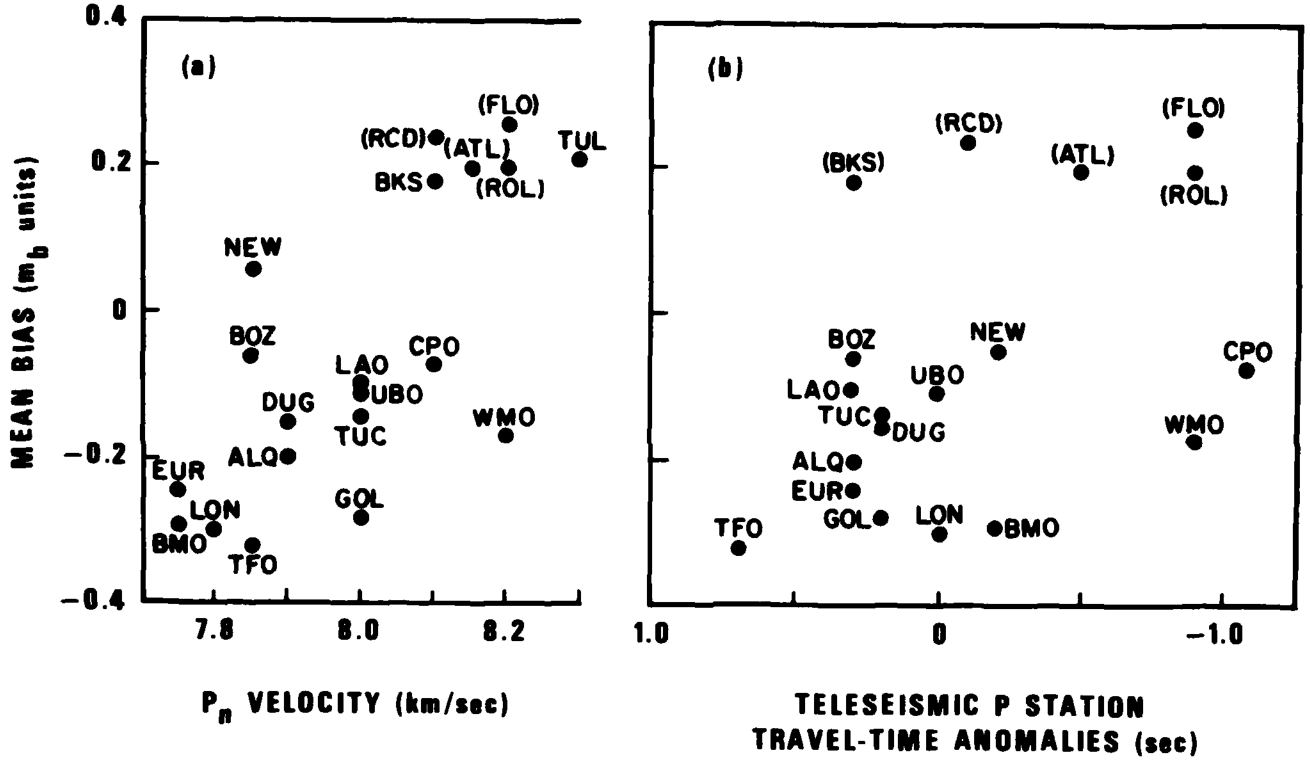

Figure 4a. Mean biases for continental US stations versus sub-station P_n velocity from Herrin (1962).

4b. Mean biases for continental US stations versus station P travel-time anomalies from Hales and Herrin (1972).

pP Corrections

Figure 5a from MSR shows the waveforms resulting from the superposition of P and pP at different delays. A more full set of superpositions may be found in Marshall (1972), from which presumably Figure 5a was drawn. Figure 5b gives the magnitude corrections, DC(T) to be added to the observed magnitude in order that the magnitude be the same as if pP had perfectly reinforced the direct wave. The correction is a function of DCR which is equal to the P-pP delay divided by the dominant period.

From a theoretical point of view, Figure 5b must be in error for small DCR--DC(T) must tend to infinity. The wave shape will go to the derivative of the direct pulse in the limit of shallow depth (DCR $\rightarrow$ 0). Thus the period will tend to a constant as DCR $\rightarrow$ 0 while the signal amplitude tends to zero. Thus the correction amplitude DC(T) should tend to infinity. As a practical matter, of course, the reflection becomes increasingly imperfect as the explosion craters and the correction must approach some limit as is suggested in Figure 5b.

Figure 5b is not complete in another respect. It is produced using a single waveform. However, over the range of magnitudes and t*'s and instrument responses of interest there are several waveforms. Figure 5c gives our calculations, (using techniques discussed in Blandford, 1976), of DC(T) for the WWSSN SP response and a granite RDP for a low frequency source (Y = 300 kt, t* = 0.6) intermediate (Y = 150 kt, t* = 0.4), and high (Y = 75 kt, t* = 0.2). The waveforms from which these figures are derived may be found in Appendix I. We see large DC(T) values for small DCR as discussed above, and appreciable (~ ± 0.07 m_b) scatter in DC(T) for any fixed value of DCR. Thus, strictly speaking, corrections should be made independently for different instrument responses and different "station" t* values.

Further complications arise when one notes that the pP reflection is not perfect. Blandford (1976) and earlier workers cited in that study showed that the typical reflection coefficient in the range around 1 Hz for NTS explosions REX, SCOTCH, and BENHAM was -0.5, and Shumway and Blandford (1977) showed that the reflection coefficient was close to -1.0 at low frequencies. Shumway and Blandford (1977) also developed a technique for producing synthetic

seismograms with a reflection coefficient which varies as a function of frequency. Using this technique, we have repeated the calculations for Figure 5 c but with a reflection coefficient equal to $-0.5(\exp(-f^2) + 1)$ where f is frequency in Hz. The results are seen in Figure 5d. Here we see an even larger scatter than in Figure 5c. Thus one concludes that the MSR correction is valid on the average but may have ~ 0.1 m_b error in any particular application.

There is good empirical evidence for the necessity of making a correction of this type. Figures 6 and 7 from Blandford et al. (1976) show variations of the "a" phase about the "c" phase (which is generally the maximum). Since the "a" phase is unaffected by pP at NTS a large value of the residual (large a) means that c has been reduced by pP, and a small residual (small a) means that c has been enhanced by pP.

In both figures the residuals are plotted versus the theoretical pP time (given by twice the depth divided by the uphole average velocity as determined from LLL data) divided by the dominant period. The dominant period was determined empirically at each station using a regression on period versus amplitude for the events in question. (It would be worth doing the plots over again using the individual period for each event.) We see that effects are large and there is a great deal of scatter, in agreement with the results in Figures 5c and 5d.

It seems to us that a more soundly based approach is needed for this problem, although the MSR technique is better than nothing.

1- Run the Shumway and Blandford (1977) maximum likelihood estimate to determine α and τ.

2- Using these α and τ values compute the synthetic waveforms for all stations--using t* as appropriate--to determine the m_b correction due to pP.

Figure 8 shows that in the magnitude range of interest (~ 70 - 300 kt), the m_b:yield slope is ~ 0.7, although in the range 2 - 70 kt the slope is close to 1.0. We have performed work to show that the analysis techniques often used bias observed slopes to smaller values if small events at different test sites are included with large events. There is every reason to suspect this problem in the MSR study at low yields. The true slope of 0.7 at large yields can combine with the biased slope < 1.0 at lower yields to

(a)

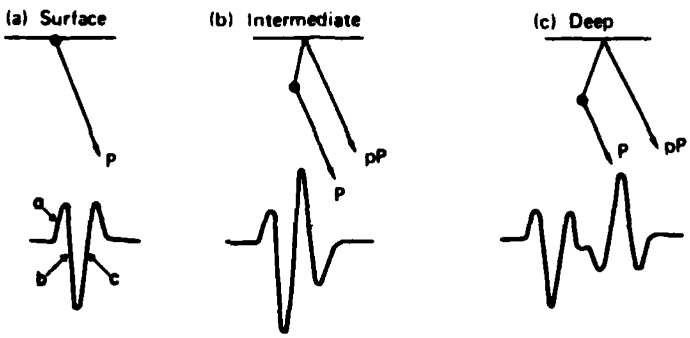

(b)

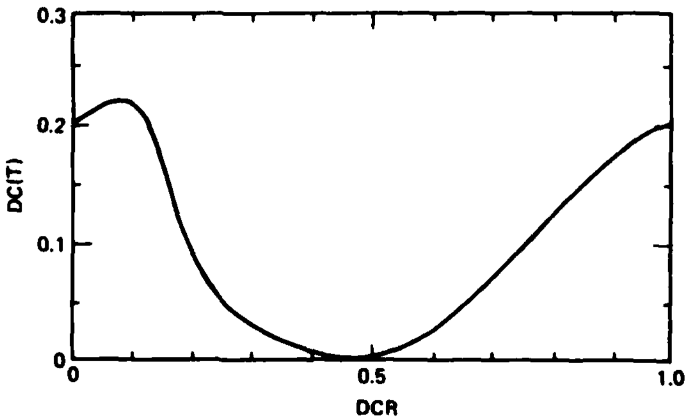

Figure 5a. Variation of the pP-P interference effect with explosion depth (from Marshall, Springer and Rodean, 1979).

5b. The magnitude-correction term DC(T) given as a function of the depth-correction ratio DCR. The DC(T) is added to magnitude to give the final magnitude m_Q (from Marshall, Springer and Rodean (1979).

(c)

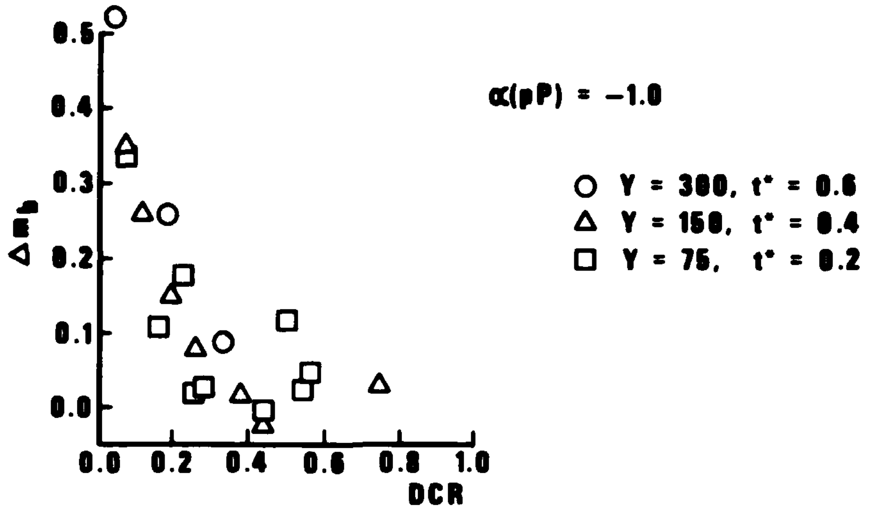

(d)

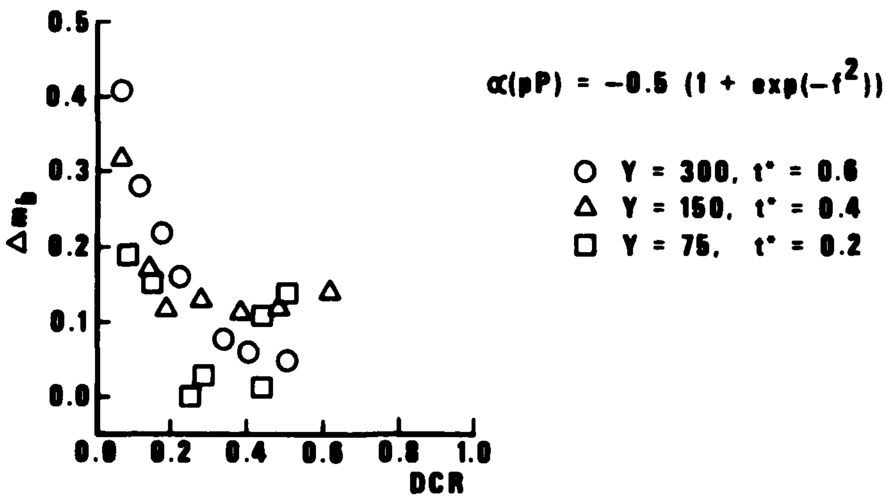

Figure 5c. Magnitude correction as a function of DCR = (pP delay/c phase period) from waveforms in Appendix I. Perfect pP reflection (αpP = -1.0), WWSSN SP response, von Seggern-Blandford granite reduced displacement potential. Correction is to be added to achieve maximum m_b possible with perfect pP enhancement for each yield.

5d. Magnitude correction as a function of DCR = (pP delay/c phase period) from waveforms in Appendix I. Variable pP reflection ($-0.5(1 + \exp(-f^2))$), WWSSN SP response, von Seggern-Blandford granite reduced displacement potential. Correction is to be added to achieve maximum m_b possible with perfect enhancement for each yield.

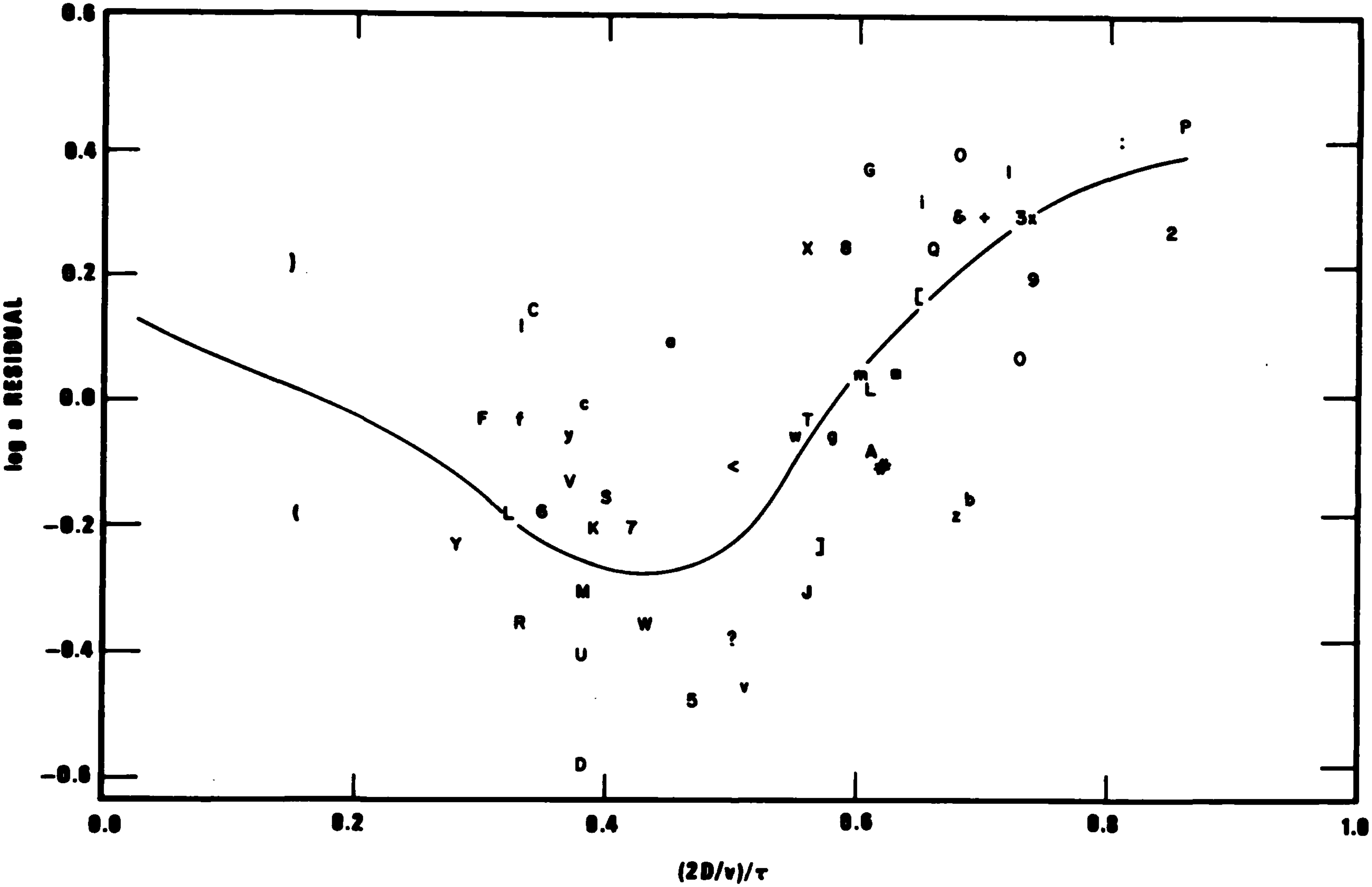

Figure 6. RKON station: Residuals of log (a) with respect to c as a function of scaled 2-way pP travel time. The solid line is hand-drawn as a subjective estimate of the main data trends (from Blandford, 1976b).

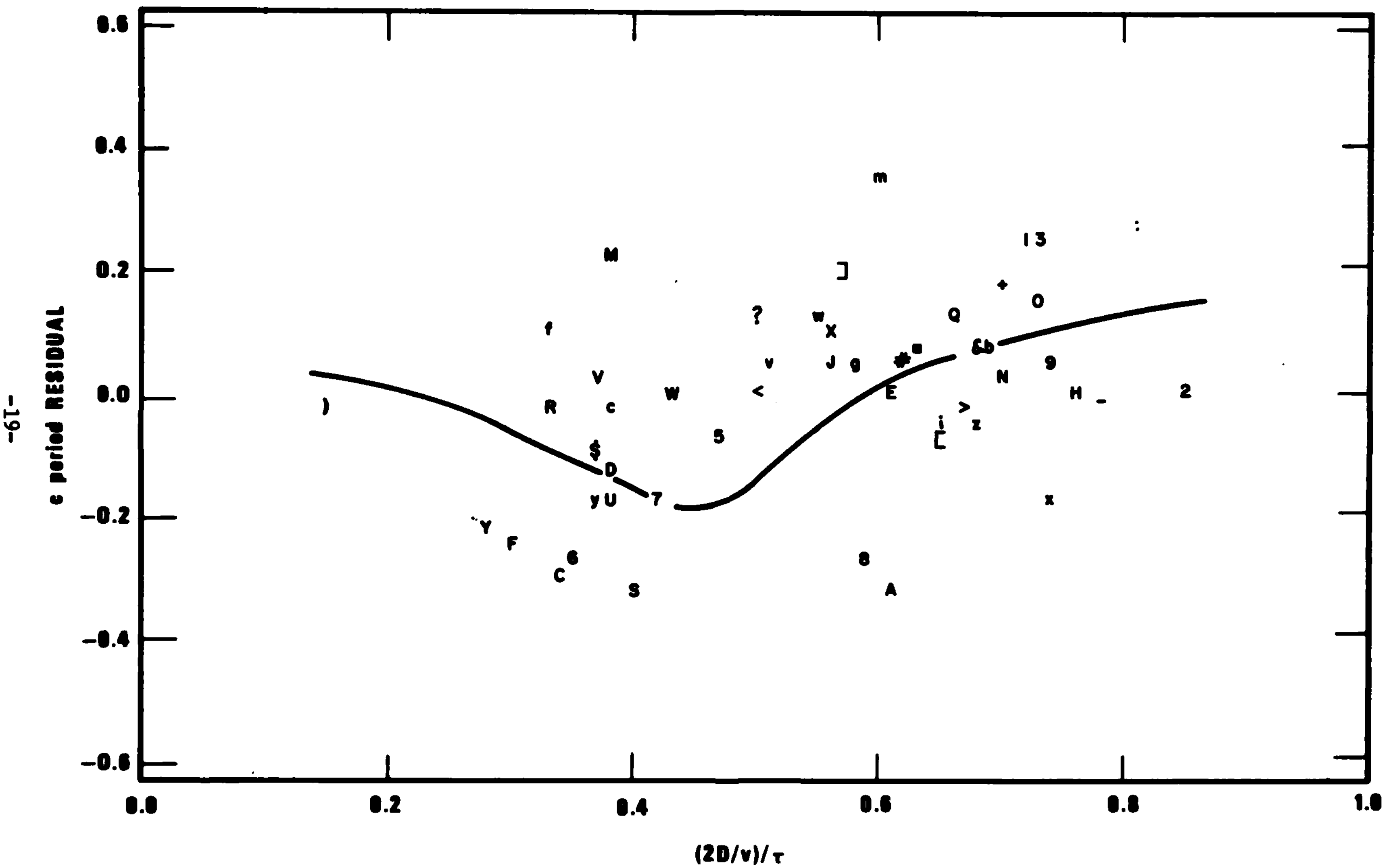

Figure 7. Residuals of log (a) at HNME with respect to c as a function of scaled 2-way pP travel time. The solid line is hand-drawn as a subjective estimate of the mean data trends (from Blandford, 1976b).

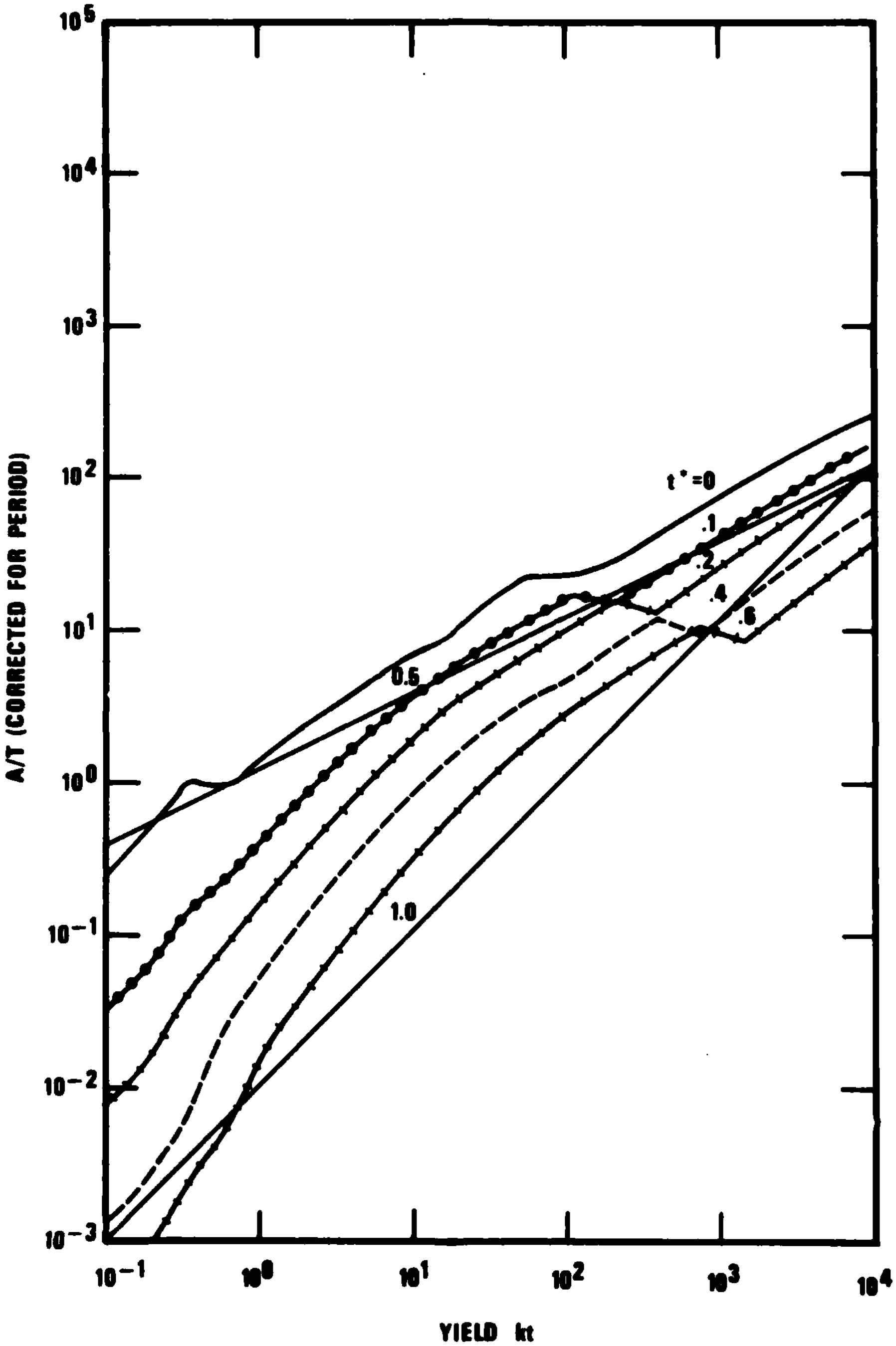

Figure 8. Theoretical amplitude-yield curves for t* = 0, 0.1, 0.2, 0.4, 0.6; granite, one-half maximum peak-to-trough amplitude for signal, corrected for LRSM instrument response at measured period, T, and divided by T, with surface reflection. pP delay equal to $0.12Y^{1/3}$ sec, with Y in kt. From Blandford (1976b).

give an (incorrect) smooth straight line of slope ~ 0.7 from low to high yields. Note that there are discontinuities in the m_b:yield curve around 100 kt due to the effects of pP in introducing "false cycles" of varying size. This suggests that in determining m_b, at shield sites especially, the period correction should not be made. (This figure is for the LRSM response. For the WWSSN response which peaks at lower frequencies, the "false cycles" are not as great a problem.)

Figure 9 plotted from waveform values in Appendix I shows directly the variation of log(c/GT) as a function of log yield for the granite reduced displacement potential, $t^* = 0.4$, $\alpha pP(f) = -0.5(1 + \exp(-f^2))$. We see that several magnitude:yield slopes are possible, depending on the variation of explosion depth (pP delay) with yield. Constant depth gives a slope in the range 0.7-0.8. If depth varies as the cube root of the yield the pP delay would vary from 0.1 sec at 75 kt to 0.16 sec at 300 kt resulting in a slope of 0.83. Slopes of 1.0 or greater are possible with different depth relations. Assuming that the pP $\geq$ 0.1 sec then the possible range in magnitude is about 0.15-0.2. For perfect pP reflections as seen in Figure 10 the range is larger 0.25-0.3, but there is no good evidence of which we are aware for such high reflection coefficients at 1 Hz.

As can be seen in Figure 11, the variation of m_b due to plausible variation in t* is much larger, approximately 0.6 magnitude units. The variations of different measures of magnitude are in parallel as a function of t* and are substantially unchanged whether measurements are made on a, c, c corrected for period:c_g, or on c corrected for period and divided by period:m_c = log(c/GT).

In Figure 11 we can see that there is, accompanying this variation, a variation which is basically undetectable on WWSSN film of the c phase period from 0.8 to 0.9 seconds. The a phase period varies more, from 0.5 to 0.8 sec; however the period of the first half-cycle is very hard to measure, and the particular parameter choice selected to be plotted has overemphasized the variation, which is more typically 0.6 to 0.8 sec. From this figure one may derive an m_b correction of $\delta m_b = 1.5\ \delta t^*$ which nicely falls near the "spectral" estimates $\delta m_b = (\pi/\log_e 10) f \delta t^*$ which gives $\delta m_b = 1.37 \delta t^*$ for T = 1, and $\delta m_b = 1.70 \delta t^*$ for T = .8.

For convenience, we have included Figures 12 and 13 which give the amplitude:yield relations for the a and c phases for perfect reflection.

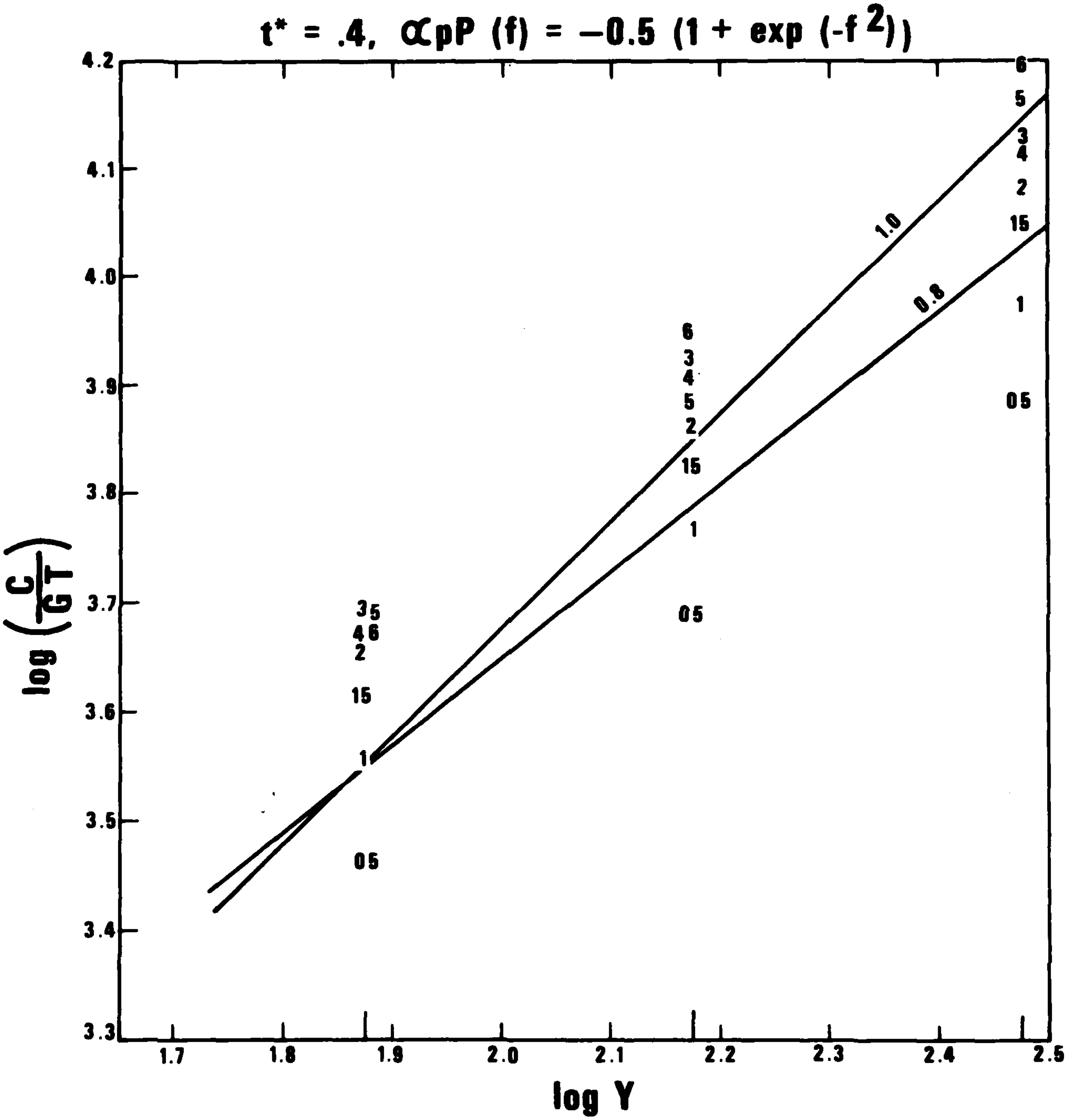

Figure 9. Theoretical amplitude:yield for $t^* = 0.4$, granite; c phase corrected for WWSSN response at measured period T, and divided by T, with surface reflection coefficient $\alpha pP(f) = -0.5(1 + \exp(-f^2))$, pP delay equal to .05, .1, .15, .2, .3, .4, .6 sec for Y = 75, 150, 300 kt. From waveforms in Appendix I.

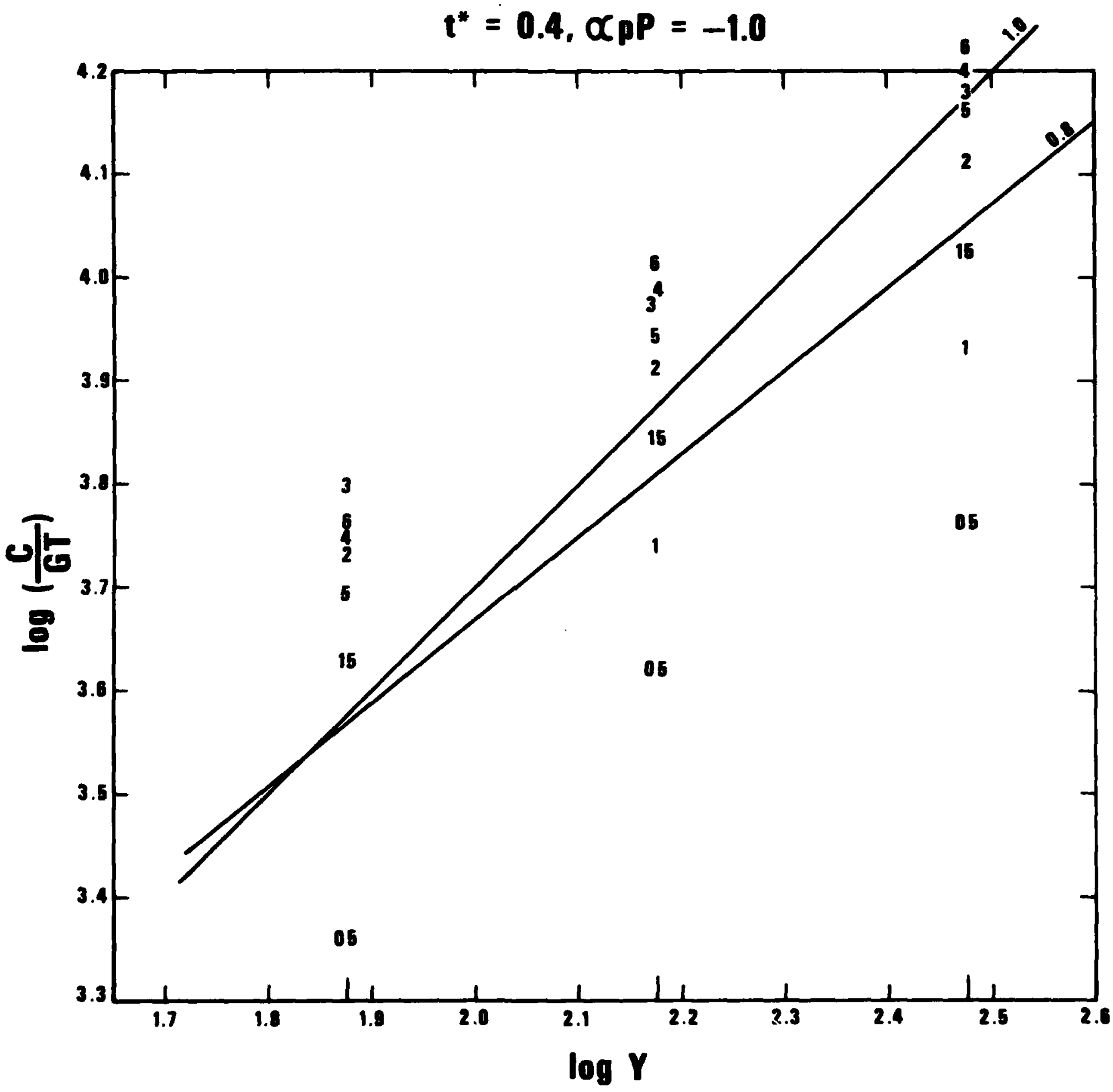

Figure 10. Theoretical amplitude:yield for t* = 0.4 granite; c phase corrected for WWSSN response at measured period T, and divided by T, with surface reflection coefficient αpP(f) = -1.0 pP delay equal to .05, .1, .15, .2, .3, .4, .6 sec for Y = 75, 150, 300 kt. From waveforms in Appendix I.

DISCUSSION AND SUGGESTIONS FOR FURTHER RESEARCH

It seems that corrections for effects of pP and absorption should be made in yield estimation and that the procedures outlined in MSR are reasonable approaches to the problem. The pP problem could be attacked in a more operational manner and with more accuracy by determining the pP delay and reflection coefficient and then computing the m_b correction directly from the appropriate synthetic waveform. The absorption problem should be attacked by further analysis of the P_n-residual correction.

Another approach to the absorption problem which seems very promising is that of determining t* from the periods of short-period S waves of deep events with plenty of high-frequency energy. This approach, in contrast to the magnitude of travel-time residual methods, does not require that the precise event location or magnitude be known or even that the absolute calibration level of the instrument be known. WWSSN data and even data reported from the AI, can be used in these determinations. The t* is determined in this approach exactly in the 1 Hz frequency band that is of greatest interest for magnitude determinations.

Other sources of error in magnitude determinations are the focusing-defocusing scatter in magnitude generated by small (20-50 km) shifts in the test site, effects of clipping and of signals below the noise level, amplification due to crustal structure at the recording site and at the source and, of course, variations in coupling due to the shot point medium.

It could be a worthwhile study to determine magnitudes for selected shots of interest including PILEDRIVER, HARDHAT, RUBIS, SAPHIRE, SALMON, and selected Soviet shots with all of the above considerations taken into account. The principal data base should be the WWSSN system with LRSM supplementation for the HARDHAT-PILEDRIVER pair, because HARDHAT occurred before much of the WWSSN system was up. AEDS data should also be analyzed in order to estimate and allow for network biases and inescapable scatter.

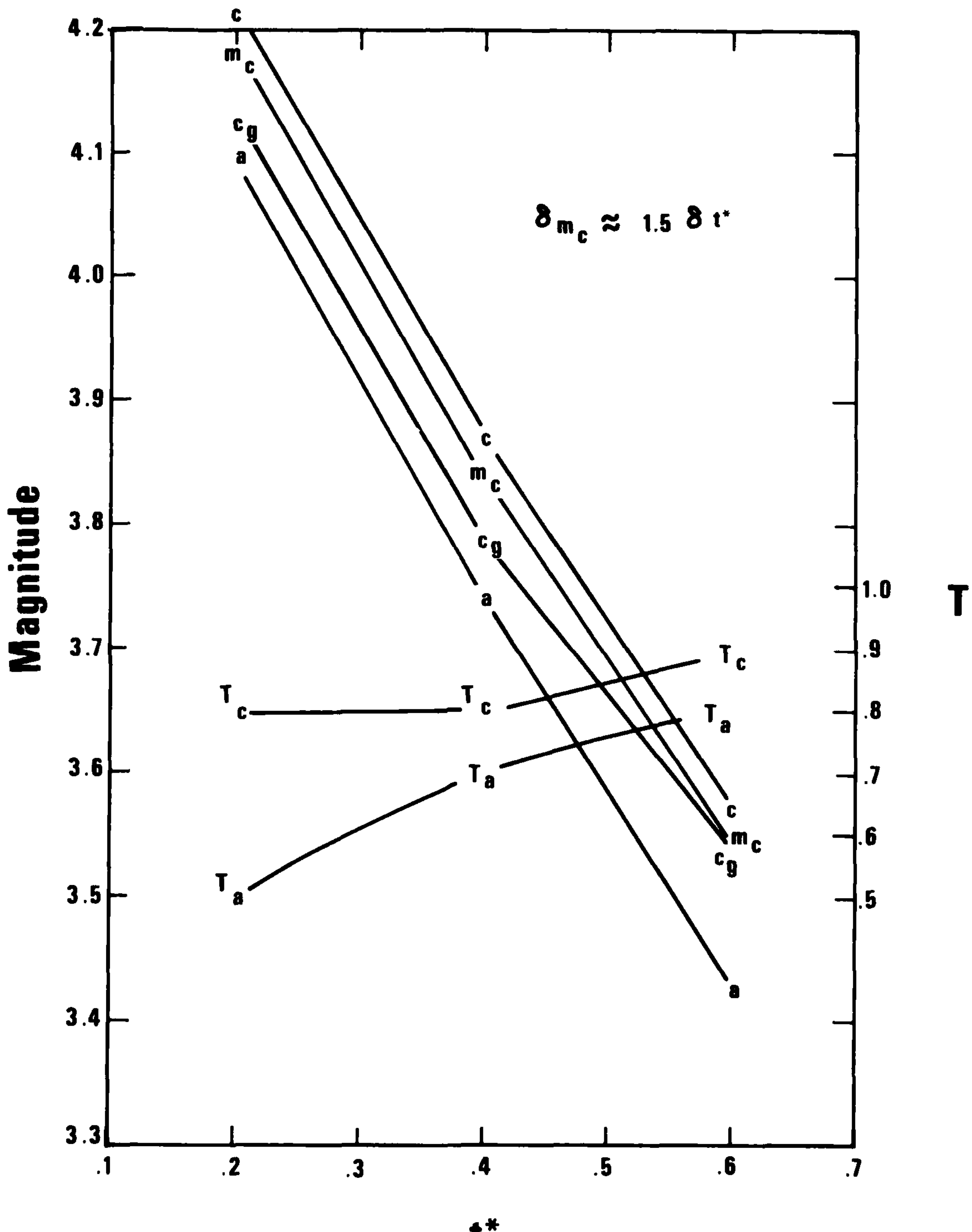

Figure 11. Theoretical curves of magnitude and period as a function of t* for several definitions of magnitude. Granite, WWSSN response surface reflection coefficients $\alpha pP(f) = -0.5(1 + \exp(-f^2))$, pP delay equals 0.15 sec, Y = 150 kt. C_g is c corrected for instrument response at period T, c/G, and m_c ub c/GT. From waveforms in Appendix I.

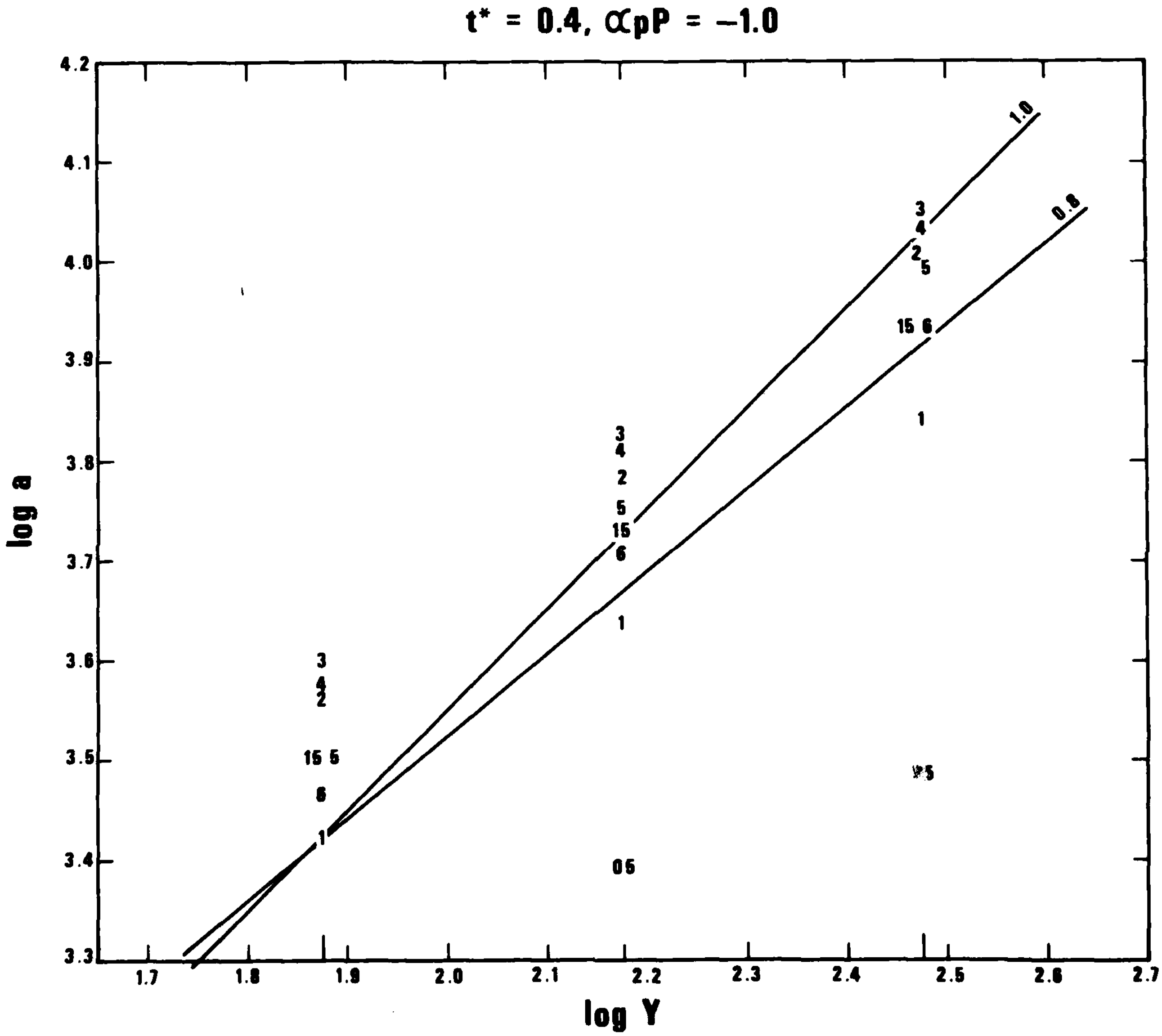

Figure 12. Theoretical amplitude:yield curves for $t^* = 0.4$ granite, a phase with surface reflection coefficient $\alpha pP(f) = -1.0$, pP delay equal to .05, .1, .15, .2, .3, .4, .6 sec for Y = 75, 150, 300 kt. From waveforms in Appendix I.

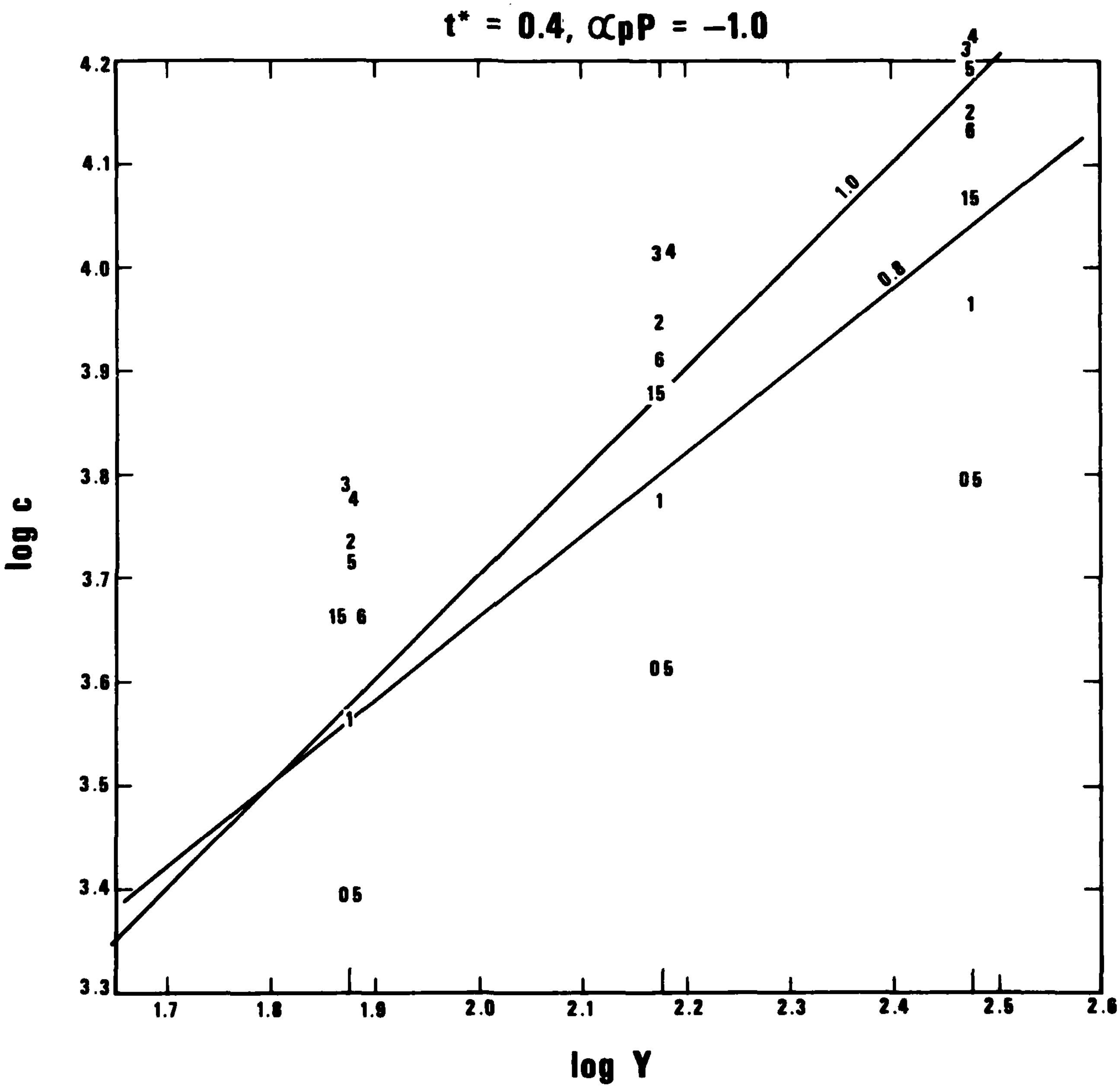

Figure 13. Theoretical amplitude:yield curves for t* = 0.4 granite, c phase with surface reflection coefficient αpP(f) = -0.1, pP delay equal to .05, .1, .15, .2, .3, .4, .6 sec for Y = 75, 150, 300 kt. From waveforms in Appendix I.

REFERENCES

Blandford, R. (1976a). Experimental determination of scaling laws for contained and cratering explosions, SDAC-TR-76-3, Teledyne Geotech, Alexandria, Virginia.

Blandford, R. (1976b). Empirical m_b:M_s relations at the Nevada Test Site with applications to m_b:yield relations, SDAC-TR-76-14, Teledyne Geotech, Alexandria, Viriginia.

Booth, D. C., Marshall, P. D. and Young, J. B. (1974). Long and short period P-wave amplitudes from earthquakes in the range 0° - 114°, Geophys. J. R. Astr. Soc., 39, 523-537.

Der, Z. A. (1977). On the existence, magnitude and causes of broad regional variations in body-wave amplitudes, SDAC-TR-76-8, Teledyne Geotech, Alexandria, Virginia.

Der, Z. A., McElfresh, T. W. and C. P. Mrazek (1979). Interpretation of short-period P-wave magnitude anomalies at selected LRSM stations, Bull. Seism. Soc. Am., 69, 1149-1160.

Der, Z. A., McElfresh, T. W. and A. O'Donnell (1980). Results of the SDCS experiment. Final Report, SDAC-TR-80-4, Teledyne Geotech, Alexandria, Virginia.

Dopp, S. (1964). Preliminary note on a refracted P phase in the western rift valley of Africa, J. Geophys. Res.,69, 3027-3031.

Hales, A. L. and E. Herrin (1972). Travel time of seismic waves, The Nature of the Solid Earth, McGraw Hill, New York.

Herrin, E. (1969). Regional variations in P-wave velocity in the upper mantle beneath North America, The Earth's Crust and Upper Mantle, Geophysical Monograph 13, 242-246.

Marshall, P. D. (1972). Some seismic results from a worldwide sample of large underground explosions, AWRE Report 049/72, Aldermaston, Berskire, England.

Marshall, P. D., Springer, D. L. and H. C. Rodean (1979). Magnitude corrections for attenuation in the upper mantle, Geophys. J. R. Astr. Soc., 57, 609-638.

North, R. G. (1977). Station magnitude bias-its determinations, causes and effects, Lincoln Laboratory, Massachusetts Inst. of Technol., 1977-24.

Searle, R. C. and P. Gouin (1971). An analysis of some local earthquake phases originating near the Afar Triple Junction, Bull. Seism. Soc. Am., 61, 1061-1071.

Shumway, R. H., and R. R. Blandford (1977). On detecting and estimating multiple arrivals from underground explosions, SDAC-TR-77-8, Teledyne Geotech, Alexandria, Virginia.

APPENDIX I

WWSSN Waveforms and Short-Period Measurements of 75, 150, 300 kt granite explosions, $t^* = 0.2, 0.4, 0.6$, pP delay .05, 0.1, 0.15, 0.2, 0.3, 0.4, 0.5, 0.6 seconds. Full and partial pP reflection coefficients.

Appendix I

This appendix contains theoretically calculated waveforms together with measurements made from those waveforms by computer. These waveforms serve as the basis for many of the plots in the body of this report. The calculation technique is to form an amplitude spectrum as the product of the von Seggern-Blandford scaled reduced displacement spectrum for granite times the WWSSN short-period instrument response and finally times $\exp(-\omega t^*/2)$. The minimum phase wavelet with this spectrum is then convolved with two delta functions representing P and pP. In the case where pP has the spectrum modified by $-0.5(1 + \exp(-f^2))$, the second delta function is replaced before convolution by the minimum phase wavelet with that spectrum.

The first set of waveforms is for perfect pP reflection ($\alpha pP = -1.0$) and the second set $\alpha pP(f) = -0.5\ (1 + \exp(-f^2))$. Yields of 75, 150, and 300 kt are put through t* values of 0.2, 0.4, and 0.6. Both the a and c phases are measured. For each waveform the upper set of four numbers is period (T), log amplitude (logA), log(A/G) where G is the gain relative to 1 Hz at period T, and logA/(GT) which is proportional to magnitude as usually defined.

The upper set of four numbers is for the a and phase the lower set is for the c phase. All the magnitudes are correct relative to each other; however, the overall absolute level has been adjusted to be in the range of typical values.

QpP = -1.0

			T log(A/G)	log A log(A/GT)	τpP = .05	T log(A/G)	log A log(A/GT)	τpP = .1
t* = .2	75 kt	a	0.60	3.90	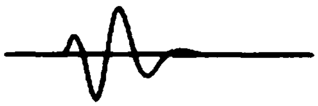	0.60	3.84	
			3.76	3.98		3.70	3.92	
		c	0.70	4.05		0.90	3.99	
			3.90	4.06		3.92	3.96	
	150 kt	a	0.70	4.12	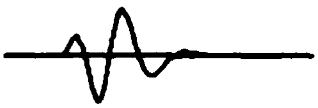	0.70	4.07	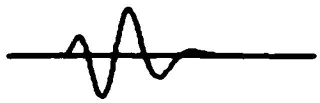
			3.98	4.13		3.93	4.08	
		c	0.70	4.27		0.80	4.22	
			4.12	4.28		4.09	4.19	
	300 kt	a	0.70	4.33	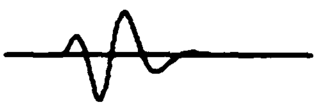	0.80	4.29	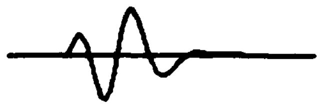
			4.19	4.34		4.16	4.26	
		c	0.80	4.47		0.80	4.43	
			4.33	4.43		4.30	4.40	
t* = .4	75 kt	a	0.70	3.56	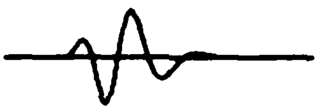	0.70	3.53	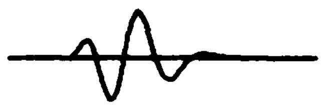
			3.42	3.57		3.38	3.54	
		c	0.80	3.72		0.90	3.70	
			3.59	3.69		3.62	3.67	
	150 kt	a	0.80	3.79	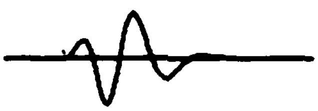	0.80	3.77	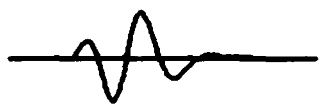
			3.66	3.76		3.64	3.74	
		c	0.80	3.95		0.90	3.94	
			3.82	3.92		3.86	3.91	
	300 kt	a	0.70	4.01	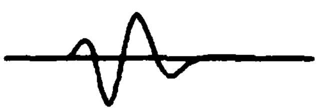	0.80	4.0	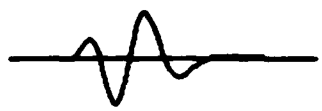
			3.87	4.02		3.87	3.97	
		c	0.90	4.16		0.90	4.16	
			4.08	4.13		4.08	4.13	
t* = .6	75 kt	a	0.80	3.26	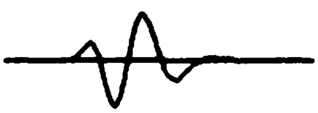	0.90	3.25	
			3.13	3.22		3.17	3.21	
		c	0.90	3.43		0.90	3.42	
			3.35	3.39		3.34	3.39	
	150 kt	a	0.80	3.51	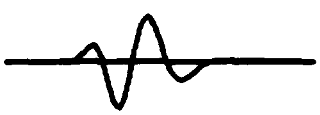	0.80	3.50	
			3.38	3.47		3.37	3.47	
		c	0.90	3.67		1.0	3.67	
			3.59	3.64		3.67	3.67	
	300 kt	a	0.80	3.73	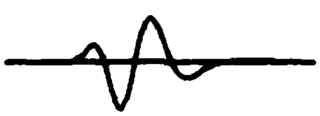	0.90	3.74	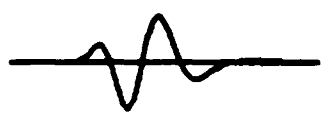
			3.60	3.70		3.66	3.71	
		c	1.0	3.88		1.0	3.90	
			3.88	3.88		3.90	3.90	

αpP = -1.0

		T / log(A/G)	log A / log(A/GT)	τpP = .3	T / log(A/G)	log A / log(A/GT)	τpP = .4
t* = .2 75 kt	a	0.60	3.90	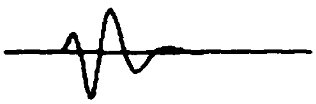	0.50	3.94	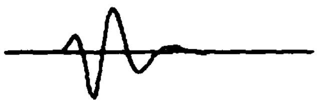
		3.76	3.98		3.85	4.15	
	c	0.60	4.04		0.70	4.10	
		3.90	4.12		3.96	4.11	
150 kt	a	0.50	4.12	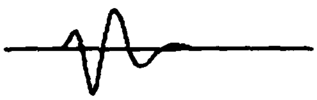	0.60	4.15	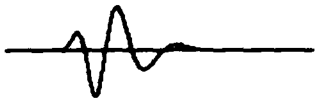
		4.03	4.33		4.01	4.23	
	c	0.70	4.24		0.60	4.30	
		4.10	4.25		4.16	4.38	
300 kt	a	0.50	4.30	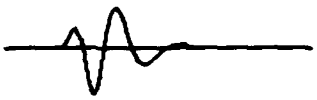	0.60	4.35	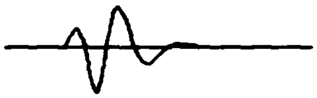
		4.21	4.51		4.21	4.44	
	c	0.80	4.41		0.70	4.48	
		4.28	4.38		4.34	4.49	
t* = .4 75 kt	a	0.60	3.50	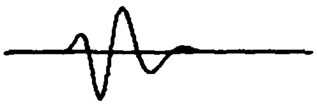	0.60	3.56	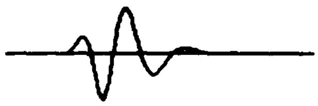
		3.36	3.59		3.42	3.65	
	c	0.80	3.66		0.70	3.73	
		3.53	3.63		3.58	3.74	
150 kt	a	0.60	3.73	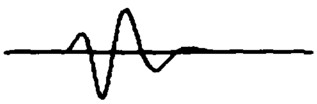	0.60	3.78	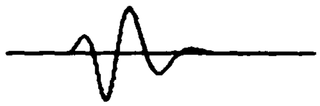
		3.59	3.82		3.65	3.87	
	c	0.80	3.88		0.80	3.94	
		3.75	3.84		3.81	3.91	
300 kt	a	0.60	3.93	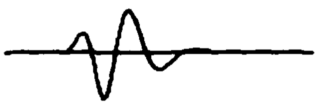	0.70	4.0	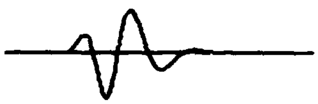
		3.79	4.02		3.85	4.01	
	c	0.80	4.06		0.80	4.14	
		3.93	4.03		4.01	4.11	
t* = .6 75 kt	a	0.60	3.16	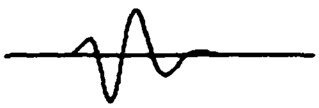	0.70	3.23	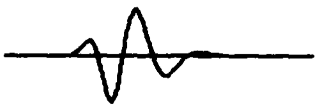
		3.02	3.24		3.08	3.24	
	c	0.80	3.32		0.80	3.40	
		3.19	3.29		3.27	3.36	
150 kt	a	0.70	3.40	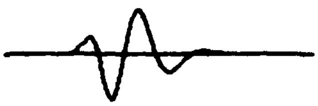	0.70	3.46	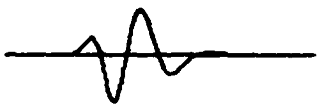
		3.26	3.41		3.32	3.47	
	c	0.80	3.55		0.90	3.62	
		3.42	3.52		3.55	3.59	
300 kt	a	0.80	3.61	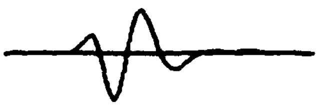	0.70	3.68	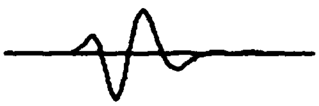
		3.48	3.58		3.54	3.69	
	c	0.80	3.75		0.90	3.83	
		3.62	3.72		3.76	3.80	

QpP = −1.0

			T log(A/G)	log A log(A/GT)	τpP = .15	T log(A/G)	log A log(A/GT)	τpP = .2
t* = .2		a	0.60	3.94		0.70	3.86	
	75 kt		3.80	4.02	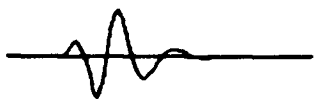	3.72	3.87	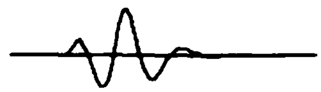
		c	0.70	4.13		0.70	4.09	
			3.99	4.14		3.94	4.10	
		a	0.70	4.16		0.70	4.11	
	150 kt		4.02	4.17	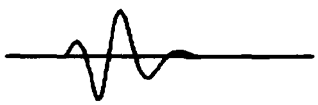	3.96	4.12	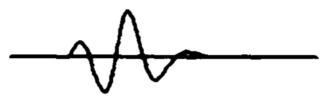
		c	0.70	4.34		0.80	4.32	
			4.20	4.35		4.19	4.28	
		a	0.70	4.37		0.80	4.33	
	300 kt		4.23	4.38	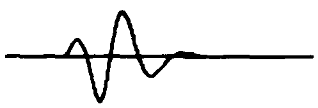	4.20	4.30	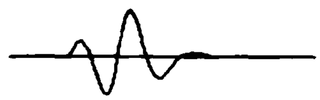
		c	0.70	4.54		0.80	4.52	
			4.39	4.55		4.39	4.49	
t* = .4		a	0.70	3.60		0.80	3.57	
	75 kt		3.45	3.61	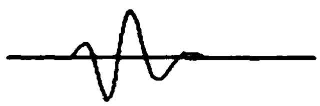	3.44	3.53	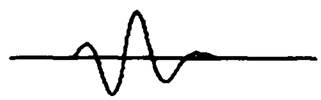
		c	0.70	3.79		0.80	3.78	
			3.64	3.80		3.65	3.75	
		a	0.70	3.83		0.80	3.81	
	150 kt		3.68	3.84	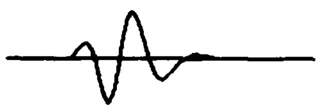	3.68	3.78	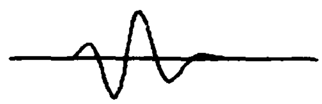
		c	0.80	4.01		0.90	4.02	
			3.88	3.98		3.94	3.99	
		a	0.70	4.05		0.80	4.04	
	300 kt		3.90	4.06	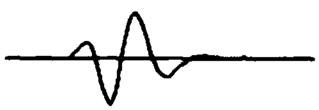	3.91	4.01	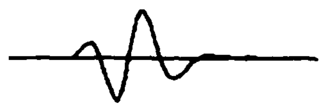
		c	0.80	4.22		0.90	4.23	
			4.09	4.18		4.15	4.20	
t* = .6		a	0.80	3.28		0.90	3.28	
	75 kt		3.15	3.25	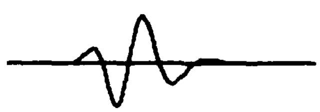	3.20	3.25	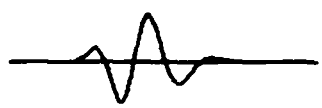
		c	0.80	3.48		0.80	3.49	
			3.35	3.44		3.36	3.46	
		a	0.70	3.53		0.80	3.54	
	150 kt		3.38	3.54	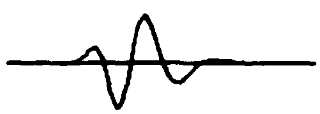	3.41	3.50	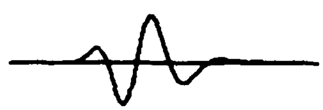
		c	0.90	3.71		0.90	3.73	
			3.63	3.68		3.66	3.70	
		a	0.80	3.76		0.90	3.77	
	300 kt		3.63	3.72	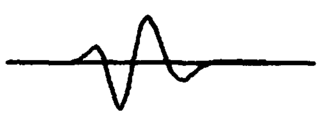	3.69	3.74	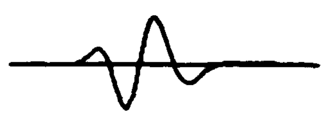
		c	0.90	3.92		0.90	3.95	
			3.85	3.89		3.88	3.92	

QpP = −1.0

			T / log(A/G)	log A / log(A/GT)	τpP = .5	T / log(A/G)	log A / log(A/GT)	τpP = .6
t* = .2	75 kt	a	0.60	3.82	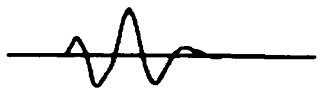	0.60	3.82	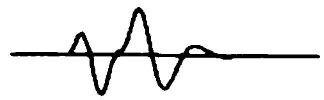
			3.68	3.90		3.68	3.90	
		c	1.0	4.02		1.20	3.96	
			4.02	4.02		4.14	4.06	
	150 kt	a	0.60	4.04	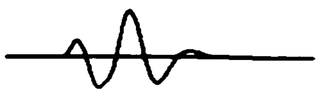	0.60	4.04	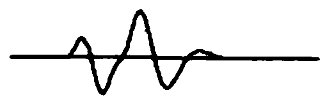
			3.90	4.12		3.90	4.12	
		c	1.10	4.25		1.20	4.20	
			4.34	4.30		4.38	4.30	
	300 kt	a	0.70	4.25	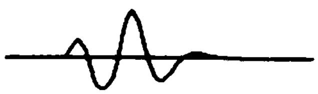	0.70	4.24	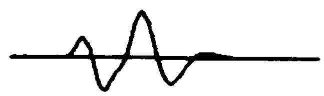
			4.10	4.26		4.10	4.25	
		c	1.0	4.45		1.20	4.41	
			4.45	4.45		4.59	4.51	
t* = .4	75 kt	a	0.80	3.50	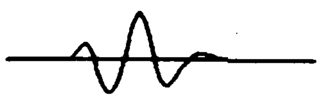	0.70	3.47	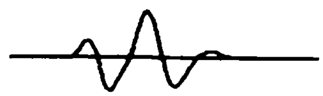
			3.37	3.47		3.33	3.48	
		c	0.90	3.72		1.20	3.67	
			3.65	3.69		3.84	3.76	
	150 kt	a	0.90	3.75	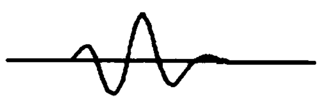	0.80	3.71	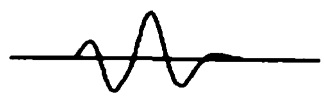
			3.67	3.72		3.58	3.67	
			0.90	3.97		1.20	3.91	
			3.89	3.94		4.09	4.01	
	300 kt	a	0.90	3.99	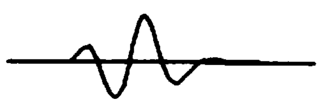	0.80	3.93	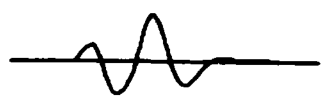
			3.91	3.96		3.80	3.90	
		c	0.90	4.19		1.20	4.13	
			4.12	4.16		4.31	4.23	
t* = .6	75 kt	a	0.90	3.24	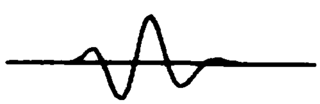	0.90	3.19	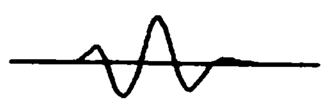
			3.16	3.21		3.11	3.15	
		c	1.0	3.46		1.10	3.40	
			3.46	3.46		3.49	3.45	
	150 kt	a	0.90	3.50	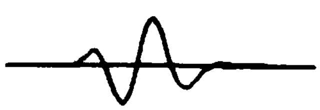	0.90	3.45	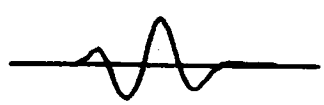
			3.43	3.47		3.37	3.42	
		c	1.0	3.72		1.10	3.66	
			3.72	3.72		3.75	3.71	
	300 kt	a	1.0	3.75	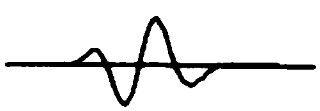	1.0	3.69	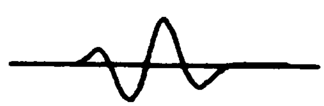
			3.75	3.75		3.70	3.70	
		c	1.0	3.94		1.10	3.90	
			3.95	3.95		3.99	3.95	

$\alpha \, pP = -0.5 \, (1 + \exp(-f^2))$

			T $\log(A/G)$	log A $\log(A/GT)$	$\tau \, pP = .05$	T $\log(A/G)$	log A $\log(A/GT)$	$\tau \, pP = .1$
t* = .2		a	0.50	3.76		0.60	3.83	
	75 kt		3.67	3.97	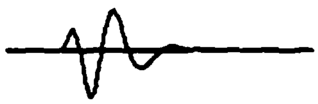	3.70	3.92	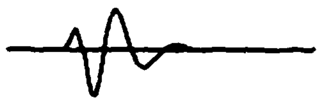
		c	0.80	3.85		0.70	3.94	
			3.72	3.82		3.80	3.95	
		a	0.60	3.96		0.50	4.05	
	150 kt		3.82	4.05	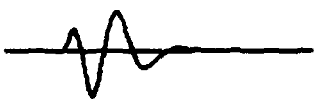	3.96	4.26	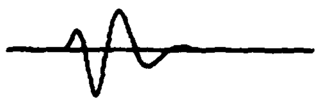
		c	0.70	4.06		0.80	4.15	
			3.92	4.07		4.02	4.12	
		a	0.50	4.15		0.60	4.24	
	300 kt		4.06	4.36	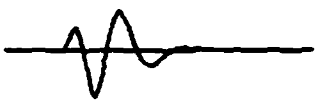	4.10	4.32	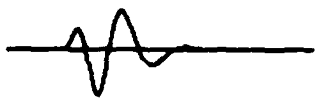
		c	0.80	4.24		0.80	4.33	
			4.11	4.21		4.20	4.30	
t* = .4		a	0.60	3.37		0.70	3.45	
	75 kt		3.23	3.45	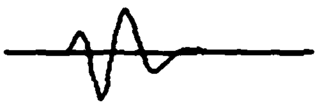	3.31	3.46	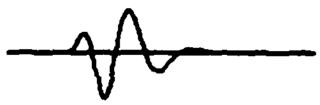
		c	0.80	3.50		0.80	3.58	
			3.37	3.46		3.45	3.55	
		a	0.70	3.59		0.60	3.68	
	150 kt		3.45	3.60	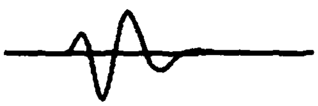	3.54	3.76	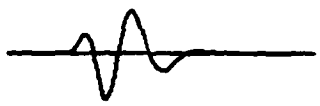
		c	0.80	3.72		0.80	3.81	
			3.59	3.69		3.68	3.77	
		a	0.70	3.80		0.70	3.89	
	300 kt		3.65	3.81	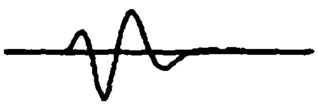	3.75	3.90	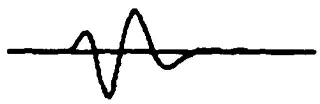
		c	0.80	3.92		0.80	4.01	
			3.79	3.88		3.88	3.97	
t* = .6		a	0.80	3.03		0.70	3.12	
	75 kt		2.90	3.0	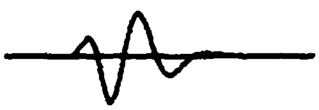	2.98	3.13	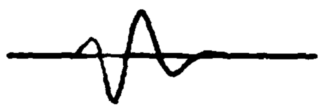
		c	0.80	3.18		0.80	3.27	
			3.05	3.14		3.14	3.24	
		a	0.70	3.28		0.70	3.36	
	150 kt		3.13	3.29	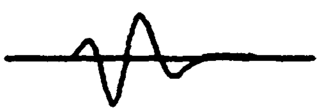	3.22	3.37	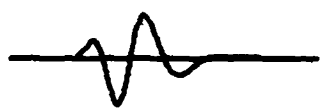
		c	0.90	3.42		0.90	3.50	
			3.34	3.39		3.42	3.47	
		a	0.80	3.50		0.80	3.59	
	300 kt		3.37	3.46	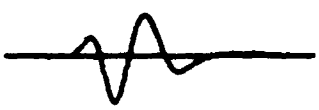	3.46	3.55	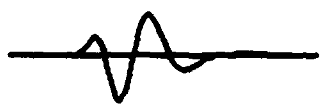
		c	0.90	3.63		1.0	3.71	
			3.55	3.60		3.72	3.72	

$\alpha pP = -0.5\ (1 + \exp(-f^2))$

t^*	Yield		T / log(A/G)	log A / log(A/GT)	τpP = .15	T / log(A/G)	log A / log(A/GT)	τpP = .2
t^* = .2	75 kt	a	0.50	3.88	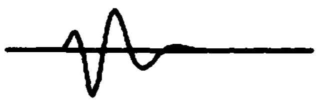	0.50	3.90	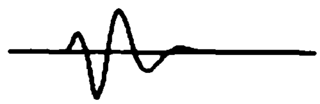
			3.79	4.10		3.81	4.12	
		c	0.70	4.01		0.70	4.04	
			3.86	4.02		3.89	4.05	
	150 kt	a	0.50	4.09	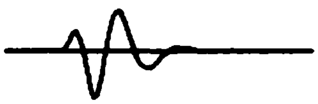	0.60	4.13	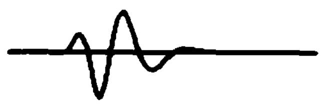
			4.0	4.31		3.99	4.21	
		c	0.80	4.21		0.70	4.25	
			4.08	4.18		4.10	4.26	
	300 kt	a	0.60	4.30	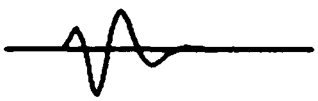	0.60	4.32	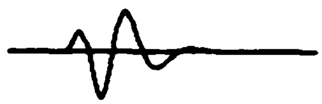
			4.16	4.38		4.18	4.40	
		c	0.80	4.40		0.80	4.44	
			4.27	4.37		4.31	4.40	
t^* = .4	75 kt	a	0.60	3.51	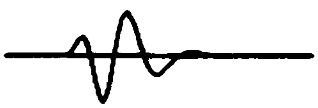	0.60	3.54	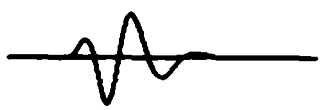
			3.37	3.59		3.40	3.63	
		c	0.80	3.65		0.80	3.69	
			3.52	3.62		3.56	3.66	
	150 kt	a	0.70	3.74	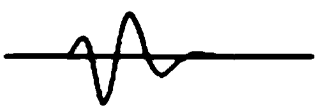	0.70	3.78	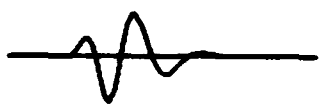
			3.59	3.75		3.63	3.79	
		c	0.80	3.87		0.80	3.92	
			3.74	3.84		3.79	3.88	
	300 kt	a	0.70	3.95	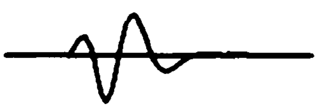	0.70	3.98	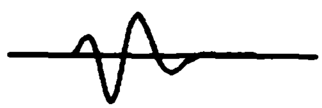
			3.81	3.96		3.84	3.99	
		c	0.90	4.07		0.90	4.11	
			4.0	4.04		4.04	4.08	
t^* = .6	75 kt	a	0.70	3.19	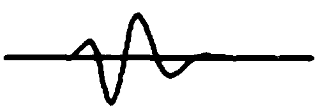	0.70	3.22	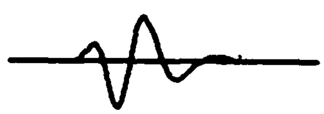
			3.04	3.20		3.08	3.23	
		c	0.90	3.33		0.90	3.38	
			3.26	3.30		3.30	3.35	
	150 kt	a	0.80	3.43	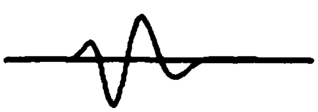	0.80	3.47	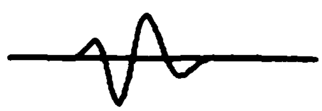
			3.30	3.39		3.34	3.43	
		c	0.90	3.57		0.90	3.62	
			3.49	3.54		3.54	3.59	
	300 kt	a	0.70	3.65	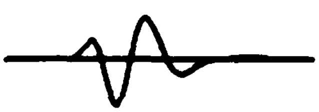	0.80	3.69	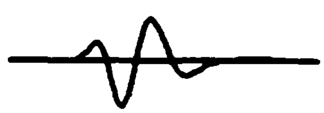
			3.50	3.66		3.56	3.66	
		c	1.0	3.78		0.90	3.83	
			3.78	3.78		3.75	3.80	

$\alpha pP = -0.5\ (1 + \exp(-f^2))$

t^*	Yield		T / $\log(A/G)$ ($\tau pP = .3$)	log A / $\log(A/GT)$ ($\tau pP = .3$)	T / $\log(A/G)$ ($\tau pP = .4$)	log A / $\log(A/GT)$ ($\tau pP = .4$)
$t^* = .2$	75 kt	a	0.50	3.84	0.60	3.82
			3.75	4.05	3.68	3.90
		c	0.60	3.95	0.60	3.79
			3.81	4.03	3.65	3.87
	150 kt	a	0.50	4.03	0.60	4.04
			3.94	4.24	3.90	4.12
		c	0.70	4.14	0.60	3.95
			4.0	4.15	3.82	4.04
	300 kt	a	0.50	4.22	0.70	4.24
			4.13	4.43	4.10	4.25
		c	0.70	4.32	0.60	4.09
			4.18	4.33	3.95	4.17
$t^* = .4$	75 kt	a	0.60	3.42	0.70	3.47
			3.28	3.50	3.33	3.48
		c	0.70	3.56	1.40	3.61
			3.42	3.57	3.95	3.80
	150 kt	a	0.60	3.63	0.80	3.70
			3.49	3.72	3.57	3.67
		c	0.80	3.77	1.40	3.86
			3.64	3.74	4.20	4.05
	300 kt	a	0.60	3.84	0.70	3.92
			3.70	3.92	3.77	3.93
		c	0.80	3.96	1.40	4.09
			3.83	3.93	4.43	4.28
$t^* = .6$	75 kt	a	0.70	3.07	0.80	3.17
			2.92	3.08	3.04	3.13
		c	0.80	3.22	1.40	3.35
			3.09	3.19	3.68	3.54
	150 kt	a	0.60	3.29	0.80	3.42
			3.15	3.37	3.29	3.39
		c	0.90	3.44	1.40	3.61
			3.37	3.41	3.95	3.80
	300 kt	a	0.70	3.51	0.90	3.65
			3.37	3.52	3.58	3.62
		c	0.90	3.65	1.40	3.85
			3.57	3.62	4.19	4.04

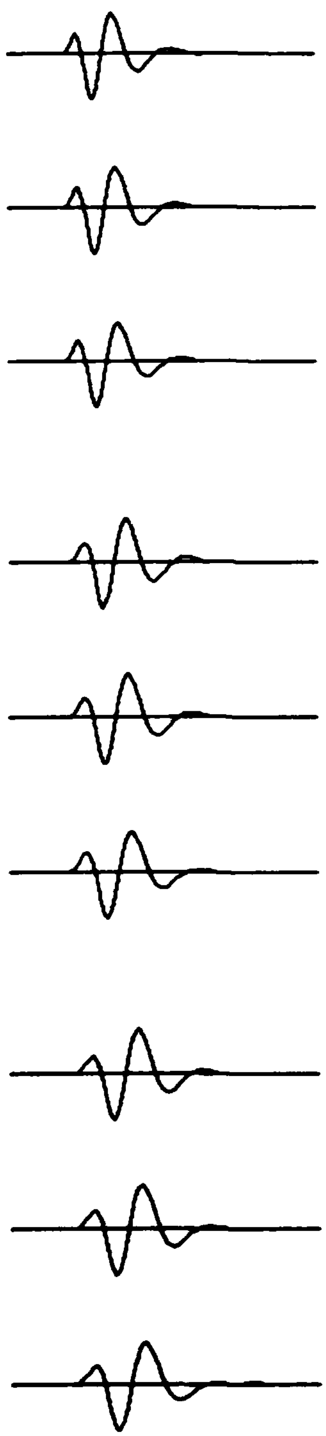

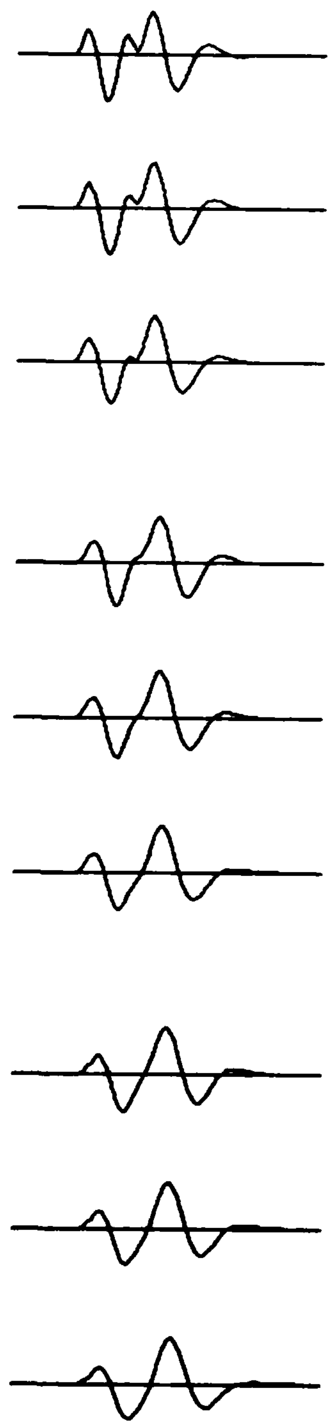

$\alpha pP = -0.5\ (1 + \exp(-f^2))$

			T log(A/G)	log A log(A/GT)	τpP = .5	T log(A/G)	log A log(A/GT)	τpP = .6
t* = .2	75 kt	a	0.60	3.82	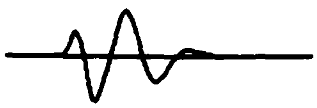	0.60	3.82	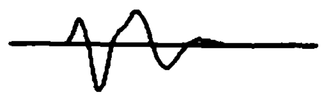
			3.68	3.90		3.68	3.90	
		c	1.0	3.93		1.20	3.86	
			3.93	3.93		4.04	3.96	
	150 kt	a	0.60	4.04	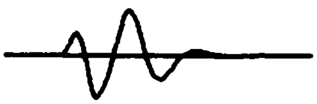	0.60	4.04	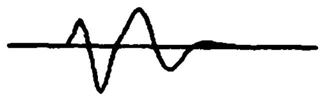
			3.90	4.12		3.90	4.12	
		c	1.10	4.17		1.30	4.11	
			4.26	4.22		4.36	4.25	
	300 kt		0.70	4.24	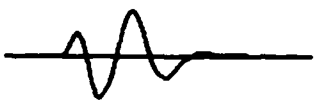	0.70	4.24	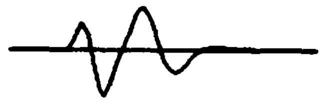
		a	4.10	4.25		4.10	4.25	
		c	1.10	4.37		1.20	4.32	
			4.46	4.42		4.50	4.42	
t* = .4	75 kt	a	0.70	3.48	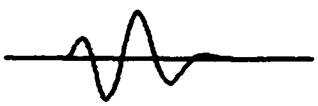	0.70	3.47	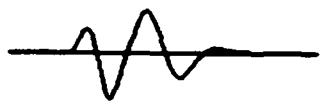
			3.34	3.49		3.33	3.48	
		c	1.10	3.64		1.20	3.58	
			3.73	3.69		3.75	3.67	
	150 kt	a	0.80	3.73	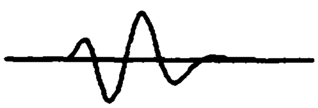	0.80	3.71	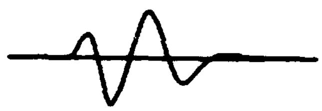
			3.60	3.70		3.58	3.67	
		c	1.0	3.89		1.20	3.83	
			3.89	3.89		4.0	3.92	
	300 kt	a	0.80	3.96	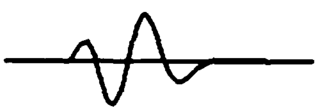	0.70	3.92	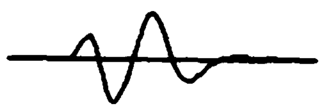
			3.83	3.92		3.78	3.93	
		c	1.10	4.11		1.30	4.06	
			4.20	4.16		4.31	4.20	
t* = .6	75 kt	a	0.90	3.21	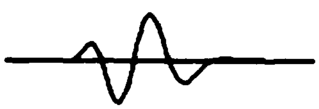	0.90	3.17	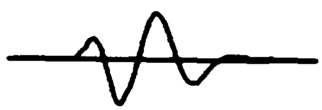
			3.13	3.18		3.10	3.14	
		c	1.0	3.38		1.20	3.32	
			3.38	3.38		3.49	3.41	
	150 kt	a	0.90	3.47	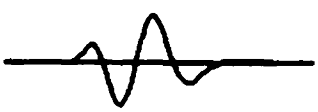	0.80	3.43	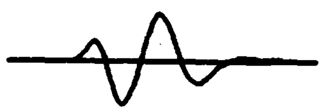
			3.39	3.44		3.30	3.40	
		c	1.0	3.64		1.30	3.58	
			3.64	3.64		3.84	3.73	
	300 kt	a	1.0	3.71	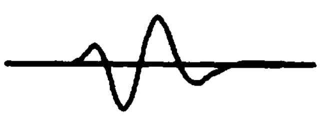	1.0	3.67	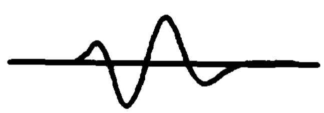
			3.71	3.71		3.67	3.67	
		c	1.0	3.87		1.20	3.82	
			3.87	3.87		4.0	3.92	